Journal of Communication Engineering (JCE)

P- ISSN: 2322-4088 Vol. 12, No. 1, Jan.-Jun. 2023 E- ISSN: 2322-3936

Characteristic Mode Analysis of Graphene Plates

K. Moradi* **[Corresponding Author]** Department of Electrical Engineering; Faculty of Energy; Kermanshah University of Technology; Kermanshah, Iran;
Email: kh.moradi@kut.ac.ir

A. Pourziad Department of Electrical and Computer Engineering; University of Tabriz; Tabriz, Iran;
Email: ali_pourziad@tabrizu.ac.ir

S. Nikmehr Department of Electrical and Computer Engineering; University of Tabriz; Tabriz, Iran;
Email: nikmehr@tabrizu.ac.ir

Received: *13 Jan. 2023* ***Revised:*** *18 Mar. 2023* ***Accepted:*** *28 Apr. 2023*

Abstract: In this paper, the resonance behavior of graphene plates with different shapes, rectangular, circular and triangular in the terahertz frequency range is analyzed with a new approach using the characteristic mode analysis. Studying the modal behavior of graphene plates leads to provide a systematic method for analyzing and designing graphene-based patch terahertz antennas, also, the parameters of graphene antennas can be obtained with simpler analyzes and better physical view. At first the effect of graphene parameters, such as chemical potential and relaxation time is studied especially on the first and second modes of the graphene plate with constant dimension. Then the effect of plate dimensions and the presence of a metal ground plane under the graphene plate on the behavior of characteristic modes is investigated. Finally, functions to calculate the resonance frequency of the plate in terms of effective parameters of the plate are presented. These functions can be used to calculate the resonance frequency in the analysis and design of graphene antennas.

Index Terms: Graphene, Characteristic Mode Analysis, Terahertz, Antenna, Resonance.

Citation: K. Moradi, A. Pourziad and S. Nikmehr, "Characteristic Mode Analysis of Graphene Plates," *Journal of Communication Engineering*, vol. 12, no. 1, pp. 67-90, Jan.-Jun. 2023.
http://dx.doi.org/10.22070/jce.2026.21170.1291

I. INTRODUCTION

Graphene, by amazing electrical properties, is the material for the miniaturization of terahertz resonant antennas [1]. Graphene, with its ability to support plasmon polariton waves in the terahertz frequency range, is a good suggestion to miniaturized and electrically adjust the antennas to make possible wireless communication between nano systems [2]. Several methods have been proposed for the analysis and design of graphene-based antennas. Among them, the characteristic mode analysis (CMA), which is a very efficient method in analyzing antennas, has often been used for metal plates or antenna structures with metal patches [3-14]. In general, if the resonant behavior and radiation performance of an antenna can be interpreted according to the concept of mode, it provides a lot of convenience in designing antennas [15]. Moreover, this method provides good physical view in studying the behavior of antennas, so similar to metal antennas, it can be an efficient method in studying graphene antennas [16]. Many graphene antennas have been proposed in literatures. They have been designed and analyzed based on various method [17-27]. Up to now a comprehensive characteristic mode analysis for graphene plate has not been proposed and this method has been applied to graphene rarely. In [28], only a rectangular graphene plate has been considered and only the effect of chemical potential on the resonance frequencies of two first mode has been studied. Also, in [29], the electromagnetic scattering characteristics of individual crumpled graphene flakes have been studied with various sizes and different levels of crumpleness. The characteristics mode analysis is used to explain the results. So the main goal of [29] is considering the effect of crumpleness in graphene flakes. Mode behavior of a graphene plate and calculating resonances from CMA point of view has not been studied in [29] and any other previous studies. The behavior of the proposed antenna in [30] is analyzed by the theory of characteristic modes. The design of the proposed antenna in [30], is based on characteristic modes theory. It is an UWB antenna with high bandwidth, different feeding and dual polarization, and consist of 4 circular monopoles placed in front of a cylindrical cavity. A wideband and slot-loaded microstrip patch antenna is presented in [6]. The bandwidth and the radiation performance of the antenna is studied by the theory of characteristic modes. In [31] the radiation efficiency and the input impedance of a graphene-based plasmonic nano-antenna is analyzed by the theory of characteristic mode. Investigation of graphene-based patch antennas in the terahertz (THz) regime using CMA has been done in [32]. The study analyzed surface current distributions and resonant modes to understand the radiation behavior and bandwidth performance. Their results demonstrate that CMA can guide the design of compact, tunable THz antennas by optimizing patch dimensions, feed position, and mode excitation, highlighting the potential of graphene for advanced THz communication and sensing applications. Despite several studies on graphene-

based antennas, the existing literature lacks a comprehensive characteristic mode analysis (CMA) that systematically evaluates how graphene's physical parameters and geometrical shapes affect modal behavior.

Previous CMA works on graphene have only focused on a single geometry or a single parameter, and primarily reported resonance shifts without providing generalized analytical models. Moreover, no prior work has compared rectangular, circular, and triangular graphene plates within a unified CMA framework, nor extracted closed-form functions to predict the resonance frequencies of fundamental modes based on chemical potential, relaxation time, and geometrical dimensions. Therefore, a rigorous and geometry-independent modal study is still missing, and such a study is essential for developing design guidelines for tunable graphene-based THz resonators and patch antennas.

In this paper, the characteristic mode analysis, is applied to graphene plates to determine the modal behavior of these plates to provide a systematic method for analyzing and designing graphene-based patch terahertz antennas. In order to investigate the effect of the ground plane, a metal plate is placed under the graphene plates. It should be noted that for electrically small structures, the first two modes are sufficient to describe the antenna resonance behavior and the other modes are high-order modes that are difficult to excite, so in most cases only the results for the first two modes are presented. This procedure has been used for graphene plates in three shapes: rectangular, circular and triangular. In all mentioned cases, the chemical potential of graphene, which is in fact a key parameter in achieving the ability to reconfigure graphene antennas, for two values of relaxation time $\tau = 0.1\ ps$ and $\tau = 1\ ps$, has been changed to investigate the effect of these two parameters on the behavior of the modes. In the studies performed in this paper, graphene is simulated as a two-dimensional impedance surface with zero thickness and temperature of 300 degrees Kelvin, in other words, the impedance boundary condition is used in its analysis. FEKO software has been used to perform the characteristic mode analysis. In some cases, an own MATLAB codes and CST software have been utilized to confirm the accuracy of the results. The results obtained from the analysis of the structures have been presented in the following three general sections: In the first part, for each of these plates, the resonance frequency and modal bandwidth of the first six modes are obtained, the current distribution and radiation patterns of these six modes are plotted. Then, the first two modes of the structure are studied and in order to analyze the radiation behavior of these two modes, the values of the three important parameters of characteristic mode analysis, namely eigenvalues, modal significance and characteristic angles, are plotted in terms of frequency. In the second part, the effect of changing two important parameters of graphene, namely chemical potential and relaxation time on the

resonance frequencies, radiation bandwidth, current distribution of modes are discussed. In the third part, the dimensions of each plate are changed for different chemical potentials to examine the effect of dimensional change on the resonance frequency according to the chemical potential variable, and finally to calculate the resonance frequency of each plate, a function according to the dimensions and chemical potential is provided.

II. THEORY

A. DRUDE MODEL

In general, since graphene is very thin (about 0.34 nm), it is usually modeled as a surface with complex surface conductivity $\sigma_g(\omega,\mu_c,\tau,T)$ and consists of two interband and intraband sections. Which is a scalar quantity in the absence of an external magnetic field and is usually expressed by the Kubo formula as relations (1) to (3) [33].

$$\sigma_g = \sigma_{inter} + \sigma_{intra} \tag{1}$$

$$\sigma_{intra}(\omega.\mu_c.\Gamma.T) = \frac{-je^2k_BT}{\pi\hbar(\omega-2j\Gamma)}\left(\frac{\mu_c}{k_BT} + 2\ln\left(e^{-\frac{\mu_c}{k_BT}}+1\right)\right) \tag{2}$$

$$\sigma_{inter}(\omega.\mu_c.\Gamma.T) = j\frac{e^2}{4\pi\hbar}\ln\left(\frac{2|\mu_c| - (\omega+2j\Gamma)\hbar}{2|\mu_c| + (\omega+2j\Gamma)\hbar}\right) \tag{3}$$

Usually in many analysis methods, graphene is considered as a thin shell and its thickness is neglected and therefore the impedance boundary condition can be considered for it. In the plate structures analyzed in this paper, graphene is modeled in two dimensions without thickness and the impedance boundary condition is used to model it.

B. SURFACE IMPEDANCE BOUNDARY CONDITION (SIBC) FOR GRAPHENE

The concepts of surface impedance were first proposed by Leontovich in 1940 and then widely used to analyze the propagation and scattering of dissipative dielectric barriers or incomplete conductors [34]. Using the surface impedance boundary condition, graphene can be simulated as a two-dimensional layer with an effective thickness small enough in a three-dimensional computational region. That is, graphene is analytically modeled as an extremely thin two-dimensional surface with a surface conductivity of σ_g [35]. By placing the graphene surface conductivity in relation to the impedance boundary condition obtained for the conductive shell, the surface boundary condition for the graphene shell is obtained as follows:

$$\hat{n} \times \left[\vec{H}_2(\omega) - \vec{H}_1(\omega)\right] = \sigma_g(\omega)\vec{E}_t(\omega) = \vec{J}_{surf} \tag{4}$$

While $\vec{H}_1$ the tangential component of is $\vec{E}_t$ are the magnetic fields on both sides of the shell, $\vec{H}_2$ the electric field on the shell, and σ_s is the surface conductivity. Also, $\hat{n}$ is the unit normal vector that is perpendicular to the surface from side 1 to side 2.

C. THE THEORY OF STRUCTURAL MODES FOR DIFFERENT GRAPHENE PLATE GEOMETRIES

To properly understand the modal behavior of graphene plates, it is essential to analyze how geometry determines the nature of the characteristics modes. Rectangular plates support two orthogonal dominant modes whose currents align with the length and width, respectively, due to the presence of two independent structural axes. Circular plates, however, exhibit degenerate modes for the first two resonances because of their rotational symmetry, leading to two orthogonal current distributions with identical resonance frequencies. In triangular plates, the modal currents strongly depend on the base-to-height ratio, and location of current maxima shifts between the vertex and the base as the geometry becomes more asymmetric. These geometry dependent mode behaviors govern how resonance frequency, bandwidth, and tunability respond to chemical potential and relaxation time. Therefore, before presenting numerical results, a structural interpretation of current flow patterns and symmetry-related mode formation is necessary for correctly understanding modal response of graphene plates.

III. RESULTS AND DISCUSSION

A. THE CHARACTERISTIC MODE ANALYSIS RESULTS FOR PLATES WITH CONSTANT DIMENSIONS AND CONSTANT CHEMICAL POTENTIAL

To analyze the characteristic mode, first three plate structures in the shapes of rectangle, circle and triangle with constant dimensions and chemical potential, $\mu_c = 0.5\ eV$ were considered. Fig. 1 shows the meshing of the three considered structures. The dimensions of the three assumed structures, the resonance frequency, and the radiation bandwidth of the first six modes are summarized in Table 1. The eigenvalue, the modal significance and the characteristic angle in terms of frequency, for the first two modes of the mentioned graphene plates and for $\mu_c = 0.5\ eV$ are shown in Figs. 2 to 7, for the rectangular, circular and triangular plate, respectively.

In these figures, the behavior of the modes has been considered close to the resonant frequency, so the graphs are plotted in the smaller frequency range. The radiation patterns of the first six modes of the above plates, ie $\vec{E}_n$ on the plane $\varphi = 0$, are also drawn in Figs. 8 to 10. The current distributions of the first six modes at the corresponding resonance frequencies are also shown in Fig. 11, for the rectangular plate, in Fig. 12, for the circular plate, and in Fig. 13, for the triangular plate. According to the current distribution, it can be seen that for the rectangular plate, it is

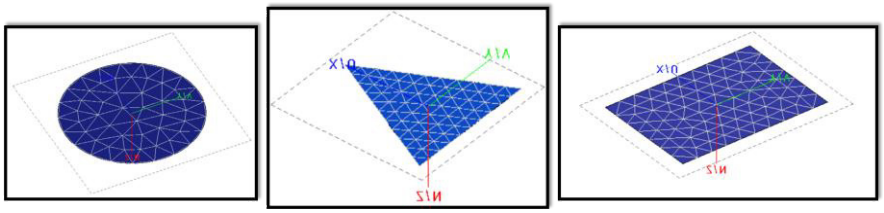

Fig. 1. Meshing of three graphene plates intended for characteristic mode analysis

generally for the first mode in the direction of horizontal flow and along the length of the plate, and its maximum intensity is at the longitudinal edges of the plate. In order to stimulate the first mode, the feed line should be applied the transverse edge or a plane wave with polarization along the length of the plate should incident on it. The current distribution of the second mode is also vertical and in line with the width of the plate, and its maximum intensity is also located at the transverse edges of the plate. Therefore, in order to stimulate the second mode, feeding should be applied to the longitudinal edge or a plane wave with polarization in the direction of the width of the plate should incident to it. The third mode also has a combination of horizontal and vertical currents of the first two modes. For the circular plate, as shown in the table of results and the distribution of currents, the resonance frequency of the first two modes of the circular plate is exactly the same, and these two modes are contiguous, one for horizontal current and the other for vertical current. Therefore, for the circular plate, instead of the first and second modes, the first and third modes are considered for study. For the triangular plate, it should be noted that the current distribution of the modes varies somewhat with the change in dimensions and depends on the height of the triangle relative to the base. According to the dimensions that the base and height of the triangle are considered equal to each other, for the first mode the direction of surface current is vertically in the direction of the height of the triangle and from the base to the vertex and its maximum intensity is close to the vertex. The direction of the second mode current is also horizontal and in line with the base of the plate, and its maximum intensity is at the edge of the base of the triangle.

Due to the change in the shape of the current distribution of the triangular plate by changing the ratio of the base to the height, for better comparison, the current distribution of the first six modes of the triangular plate whose base to height ratio is greater than one and equal to 1.5 or less One and equal to 0.5 are also shown in Figs. 14 and 15, respectively.

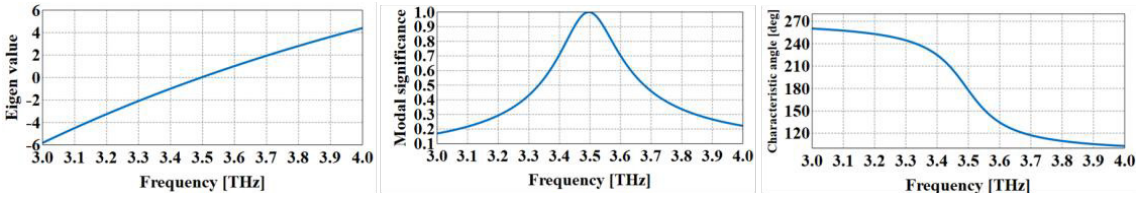

Fig. 2. The eigenvalue, the modal significance and the characteristic angle for the first mode of the rectangular plate

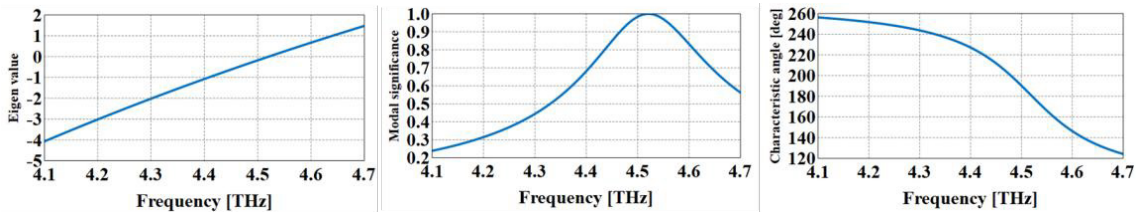

Fig. 3. The eigenvalue, the modal significance and the characteristic angle for the second mode of the rectangular plate

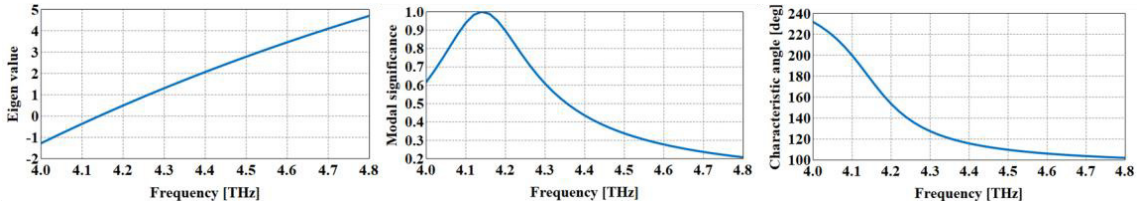

Fig. 4. The eigenvalue, the modal significance and the characteristic angle for the first mode of the circular plate

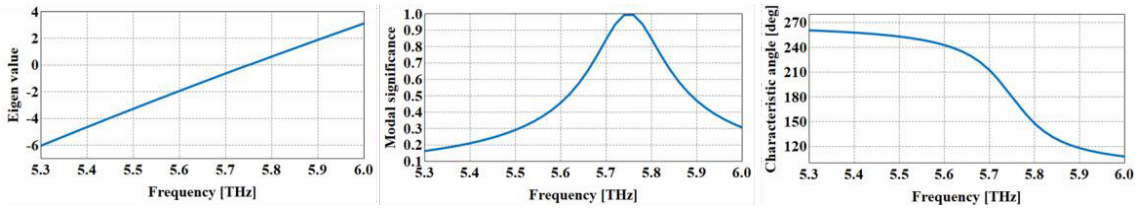

Fig. 5. The eigenvalue, the modal significance and the characteristic angle for the second mode of the circular plate

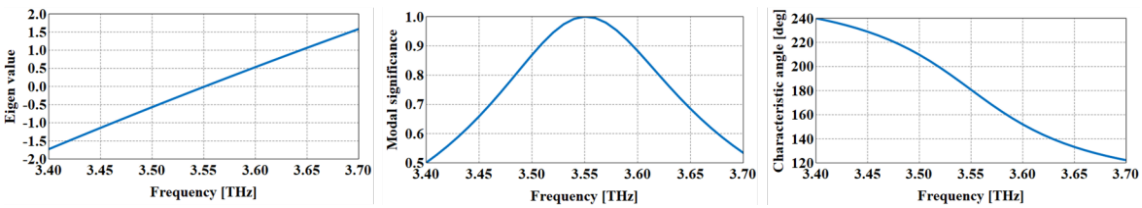

Fig. 6. The eigenvalue, the modal significance and the characteristic angle for the first mode of the triangular plate

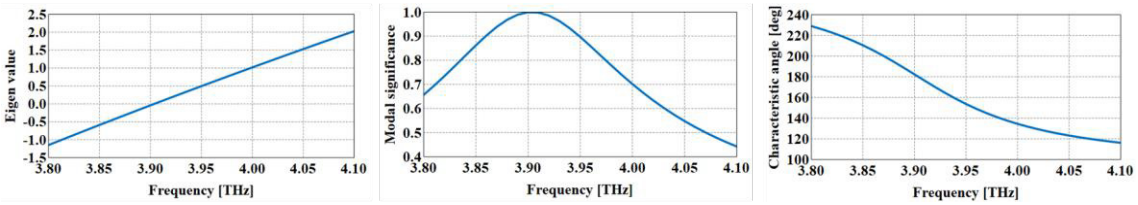

Fig. 7. The eigenvalue, the modal significance and the characteristic angle for the second mode of the triangular plate

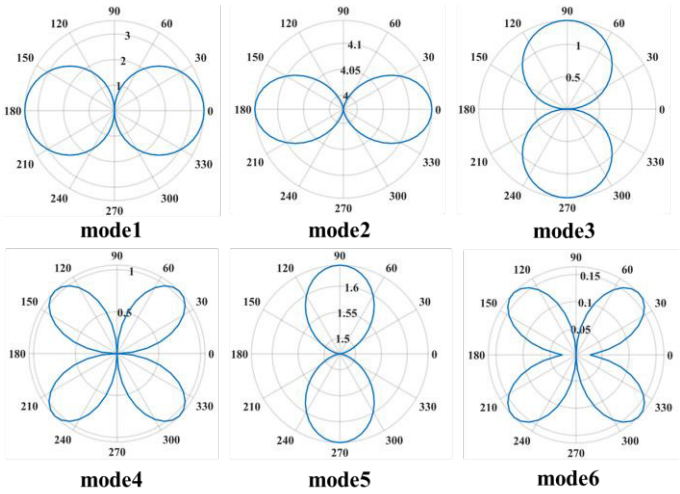

Fig. 8. Radiation patterns in the *XZ* plane for the first six modes of the rectangular plate

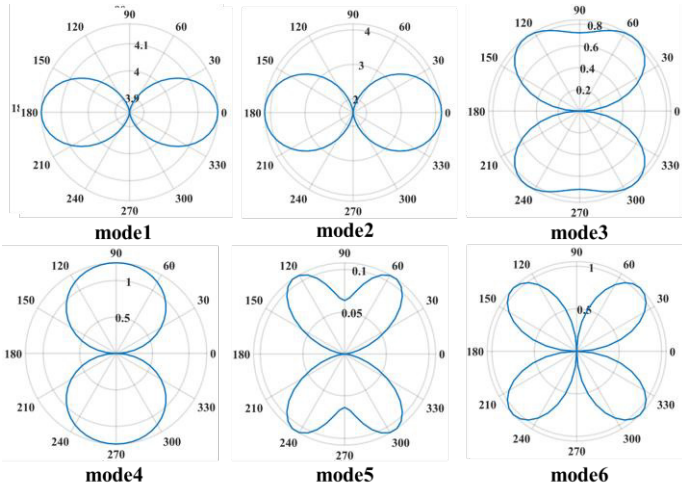

Fig. 9. Radiation patterns in the *XZ* plane for the first six modes of the circular plate

B. THE EFFECT OF GRAPHENE PARAMETERS ON THE BEHAVIOR OF MODES

In this section, the effect of two parameters of graphene, namely chemical potential and relaxation time, on the resonance frequency of modes and their radiation bandwidth are discussed. The plates are according to Fig. *1*, and their dimension according to Table 1.

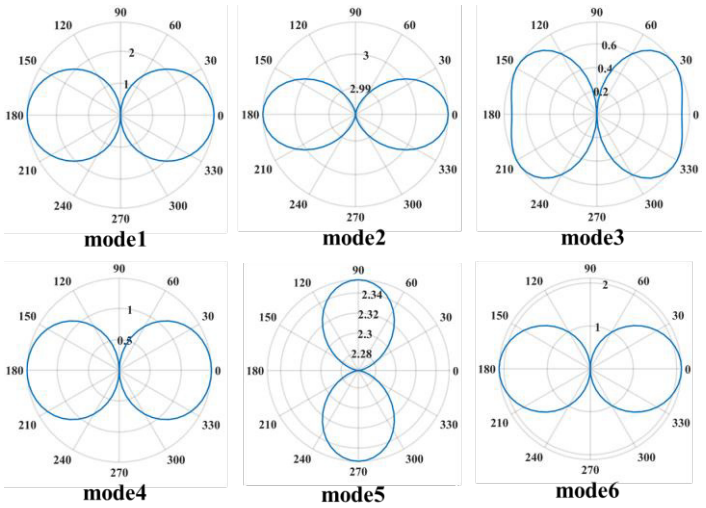

Fig. 10. Radiation patterns in the *XZ* plane for the first six modes of the triangular plate

Table 1. Resonance frequency and radiation bandwidth of the first six modes of graphene plates

		Mode 1	Mode 2	Mode 3	Mode 4	Mode 5	Mode 6
Rectangular plate Length = 10μn width = 7μn	Resonance frequency (THz)	3.5	4.52	4.93	5.92	6.4	7.31
	radiation bandwidth (%)	5.7	5.1	3	2.7	2.5	2.2
Circular plate radius = 5μn	Resonance frequency (THz)	4.14	4.14	5.75	5.75	6.95	7.47
	radiation bandwidth (%)	5.55	5.55	2.6	2.16	2.14	2.01
Triangular plate base = 10μn height = 10μn	Resonance frequency (THz)	3.55	3.9	5.5	6.39	6.54	7.34
	radiation bandwidth (%)	5.07	4.87	2.91	2.5	2.6	2.45

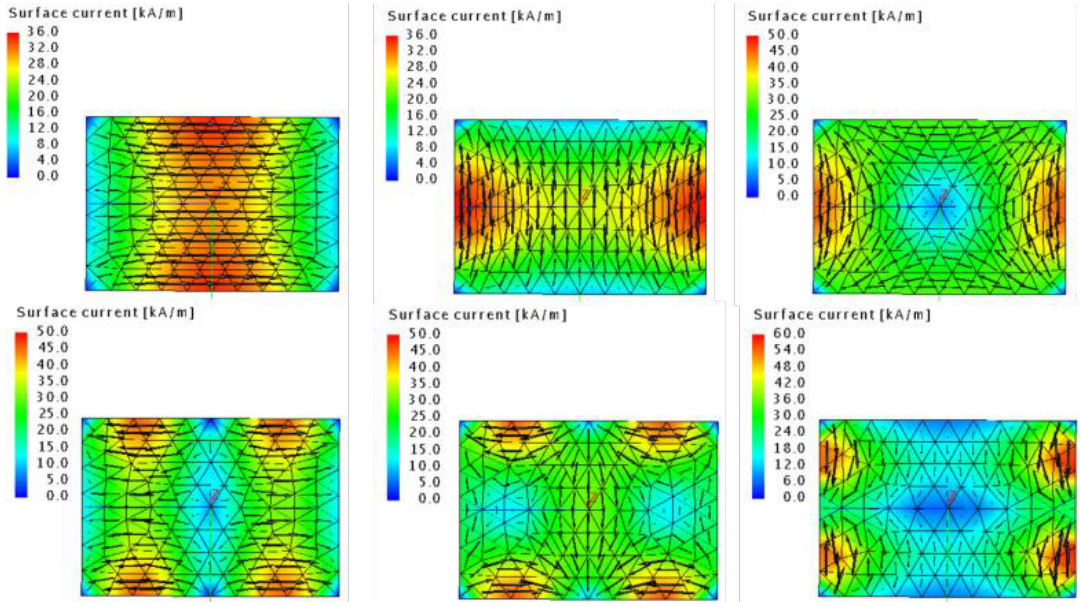

Fig. 11. Current distribution at the resonance frequencies of the first six modes of the rectangular plate

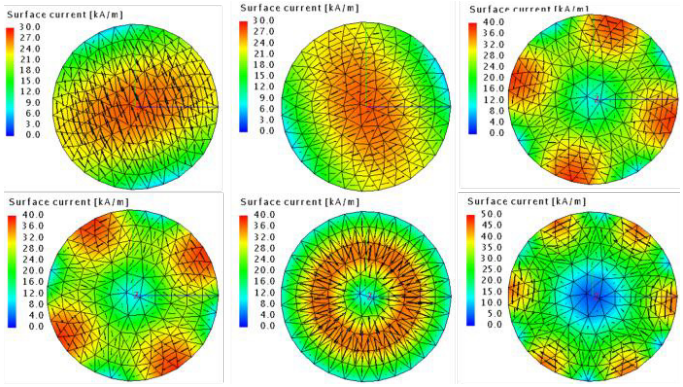

Fig. 12. Current distribution at the resonance frequencies of the first six modes of the circular plate

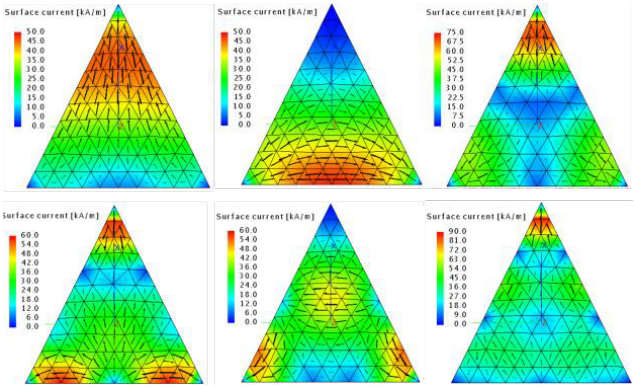

Fig. 13. Current distribution at the resonance frequencies of the first six modes of the triangular plate with 1 base to height ratio

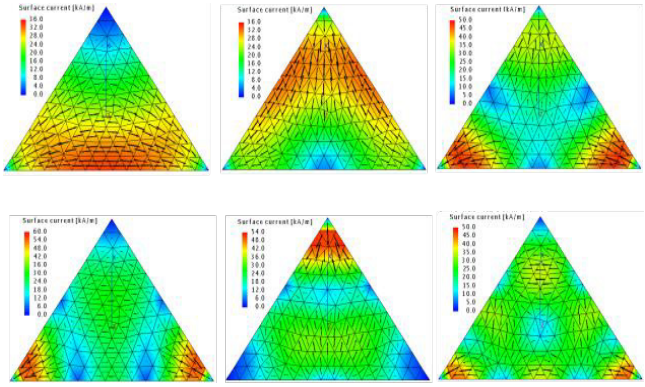

Fig. 14. Current distribution at the resonance frequencies of the first six modes of the triangular plate with 1.5 base to height ratio

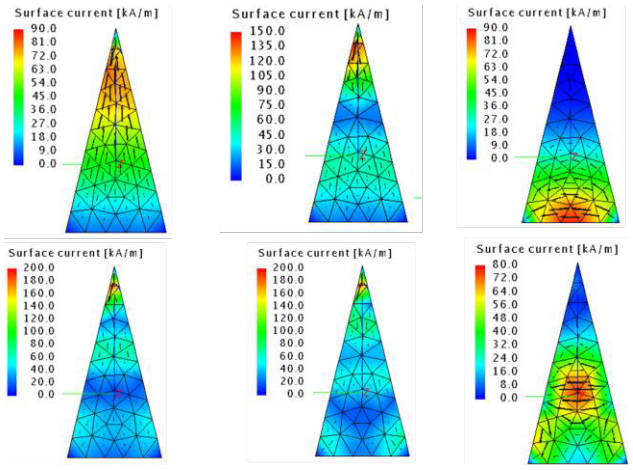

Fig. 15. Current distribution at the resonance frequencies of the first six modes of the triangular plate with 0.5 base to height ratio

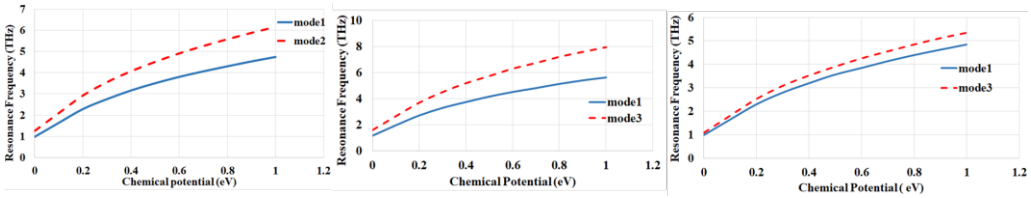

Fig. 16. Resonance frequencies of the first two modes of a) the rectangular plate, b) the circular plate, c) the triangular plate, in terms of the chemical potential of graphene

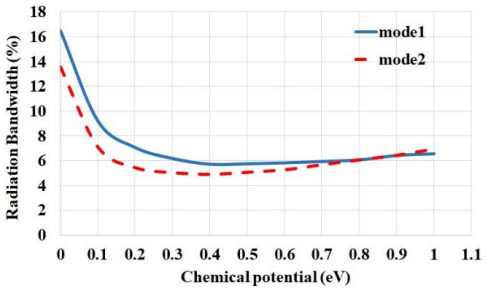

Fig. 17. Radiation bandwidth of the first two modes of the 10 µm × 7µm rectangular plate in terms of the chemical potential of graphene

B.1 THE EFFECT OF CHEMICAL POTENTIAL

The chemical potential parameter of graphene, which is the most important factor for the adjustability of graphene plates, was changed between 0 eV to 1eV. In order to better understand the effect of graphene chemical potential on the characteristic modes of the plate, the resonance frequency of the first two modes of rectangular, circular and triangular plates, versus chemical potential, are plotted in Figs. 16 to 18, respectively. These diagrams show that the resonance frequency of the modes increases with increasing chemical potential for all three structures.

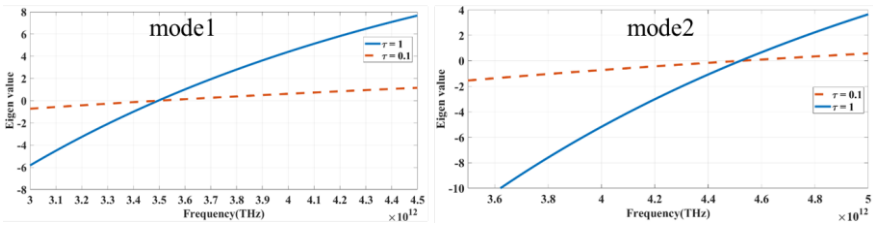

Fig. 18. The eigenvalue of the first two modes of the rectangular plate for $\tau = 0.1ps$ and $\tau = 1ps$

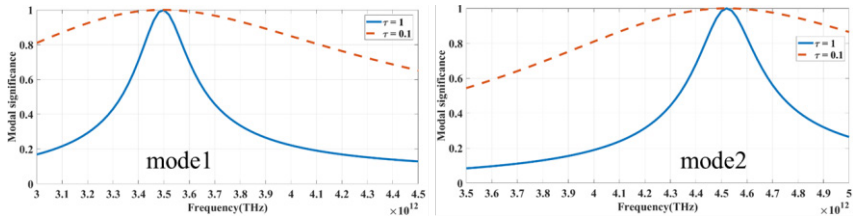

Fig. 19. The modal significance of the first two modes of the rectangular plate for $\tau = 0.1ps$ and $\tau = 1ps$

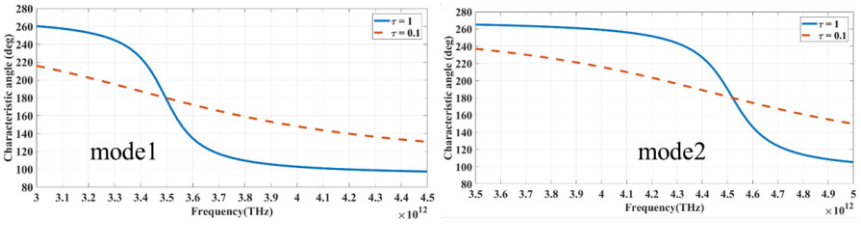

Fig. 20. The characteristic angle of the first two modes of the rectangular plate for $\tau = 0.1ps$ and $\tau = 1ps$

This upward trend is due to this fact, when the chemical potential increase, the actual surface conductivity of the graphene increase, causing the resonant frequencies of the first two modes, shift to higher frequencies. As can be seen from the diagrams in Fig. 16, the trend of changes is almost the same for both modes, and it can be said that the chemical potential of graphene will have a relatively equal effect on the resonant frequency of the first two modes of graphene plate. In order to better investigate the effect of chemical potential parameter on the radiation bandwidth of the modes, the changes in the radiation bandwidth in terms of chemical potentials for the first and second modes of the rectangular plate are shown in Fig. 17. As it turns out, with increasing chemical potential, the radiation bandwidth of both modes first decreases and then remains almost constant.

B.2 THE EFFECT OF RELAXATION TIME

Given that the effect of the relaxation time parameter on the proposed plates is the same, so only the results related to the rectangular plate will be presented. To better understand the effect of the graphene relaxation time parameter on the modes, the eigenvalue, the modal significance and the

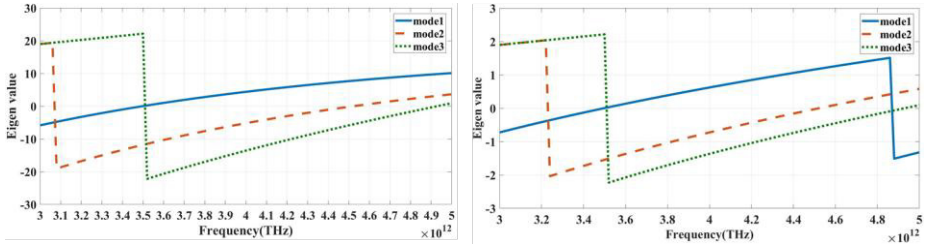

(a) (b)

Fig. 21. The eigenvalue of the first three modes of the rectangular plate for a) $\tau = 1ps$, b) $\tau = 0.1ps$

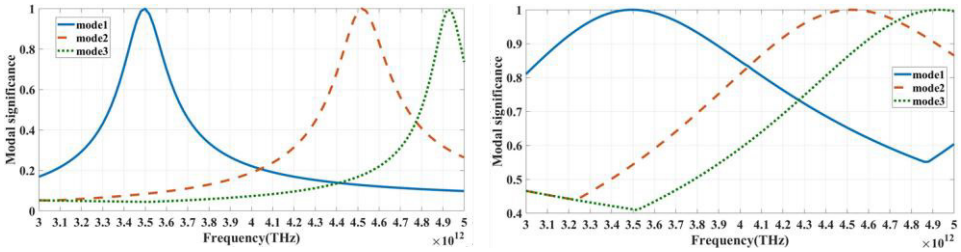

(a) (b)

Fig. 22. The modal significance of the first three modes of the rectangular plate for a) $\tau = 1ps$, b) $\tau = 0.1ps$

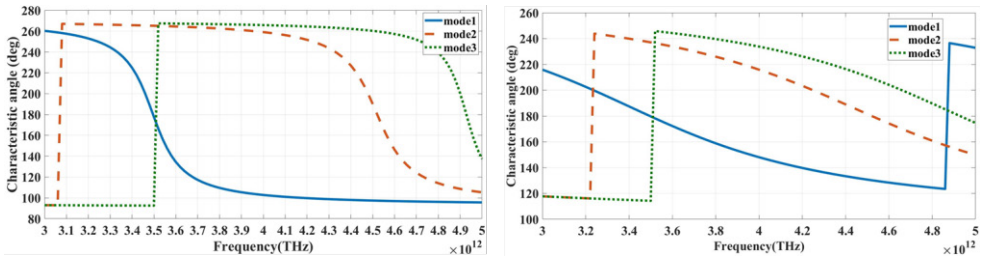

(a) (b)

Fig. 23. The characteristic angle of the first three modes of the rectangular plate for a) $\tau = 1ps$, b) $\tau = 0.1ps$

characteristic angle of the first two modes of the rectangular plate for $\tau = 1$ *ps* and $\tau = 0.1$ *ps* are displayed in Figs. 18 to 20. It can be seen from the results, that changing the location of the resonant frequencies does not change with τ, but $\tau = 1$ *ps* produces narrower resonances than $\tau = 0.1$ *ps*, so in general for $\tau = 1$ *ps*, the adjacent modes are more differentiated and are easier to detect, but for $\tau = 0.1$ *ps* the modes have more bandwidth. Comparing the graphs, we can see that the slope of the eigenvalue curve near the resonance for the state $\tau = 0.1$ *ps* is much less than the slope of the characteristic value curve at $\tau = 1$ *ps*, and this indicates less bandwidth for $\tau = 1$ *ps*.

Also, as can be seen from the characteristic angle diagrams, for $\tau = 0.1$ *ps*, the characteristic angles of both modes are close to the resonance and remains in the range of about 180 degrees. In general, the resistance of graphene is proportional to the inverse of the relaxation time τ, and a higher τ leads to a lower resistance and consequently less losses. So we can say that higher τ means higher quality graphene and sharper resonances. Since the relaxation time of graphene

Table 2. Radiation bandwidth of the first six modes of the rectangular plate for $\tau = 1ps$, $\tau = 0.1ps$

	Radiation bandwidth (%)					
	Mode 1	**Mode 2**	**Mode 3**	**Mode 4**	**Mode 5**	**Mode 6**
$\tau = 0.1$ *ps*	43	35	31	18.4	16.3	21.8
$\tau = 1$ *ps*	5.7	5.1	3	2.7	2.5	2.2

Table 3. Resonance frequency function of the first two modes of graphene plate according to the chemical potential of graphene and plate dimensions

	Resonance frequency of the first mode (THz)	**Resonance frequency of the second mode (THz)**
Rectangular plate	$\overline{f_{r1}(\mu_c, l, w) = 18.43\ \mu_c^{0.45} l^{-0.73} w^{0.18}}$	$\overline{f_{r2}(\mu_c, l, w) = 18.05\ \mu_c^{0.5} l^{0.056} w^{-0.6}}$
Circular plate	$\overline{f_{r1}(\mu_c, R) = 14.762\ R^{-0.5} \mu_c^{0.45}}$	$\overline{f_{r2}(\mu_c, R) = 21.069\ R^{-0.5} \mu_c^{0.45}}$

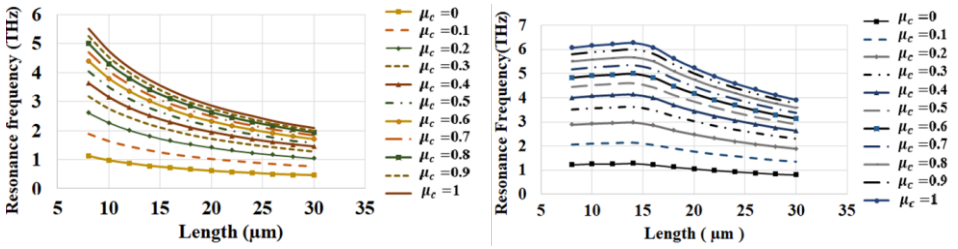

(a) (b)

Fig. 24. Resonance frequencies of the rectangular graphene plate as a function of plate length for (a) the first mode, (b) the second mode

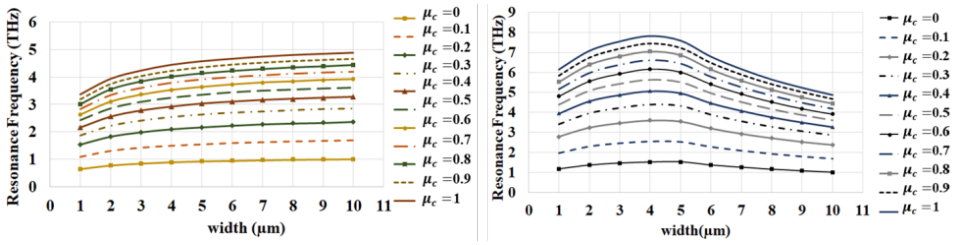

(a) (b)

Fig. 25. Resonance frequencies of the rectangular graphene plate as a function of plate width for (a) the first mode, (b) the second mode

affects the bandwidth, in order to better investigate the effect of this parameter on the radiation behavior of the modes, the radiation bandwidth of the first six modes for a rectangular plate with $\tau = 0.1$ *ps* is extracted and calculated from the graphs and for better comparison, they are presented in Table 2, next to the bandwidth of the plate with $\tau = 1$ *ps*. Also, in order to better understand the behavior of the first three modes next to each other and compare them, a diagram of the three parameters of eigenvalue, modal significance and characteristic angle of the first three modes is drawn after applying mode tracking in Figs. 21 to 23.

B.3 THE EFFECT OF DIMENSION ON THE BEHAVIOR OF MODES

In order to investigate the effect of dimensions on the resonances of the first and second modes of the graphene plate, the length and width of the rectangular plate, the radius of the circular plate and the base and height of the triangular plate were changed for different chemical potentials. The results obtained for the first two modes of each plate are summarized in Tables 3 and 4.

Rectangular Plate: The resonance frequencies of the first two modes of the rectangular plate in terms of plate length (L) and in terms of plate width (W) for different chemical potentials (μ_c) have been shown in Figs. 24 and 25, Respectively. As can be seen from the graphs, as the plate length increases, the resonant frequency of the first mode generally increases, but the resonance of the second mode remains almost constant at first and then decreases with further increase in plate length.

Thus, it is clear that the resonance of the second mode depends more on the length-to-width ratio of the plate than on the width itself. Also, according to the slope of the graphs, it can be seen that the effect of length is on the first mode and has little effect on the second mode. Also, by increasing the width of the plate, the resonance of the first mode increases with a much smaller slope than the change of length and will remain almost constant, while the change of width will have a greater effect on the second mode. Both in the ascending and descending parts (due to the length to width ratio), there is a greater slope than changing the resonances of this mode by changing the length. On the other hand, by increasing the chemical potential for each plate with constant dimensions, the resonance frequency of both modes with a trend of approximately Increases the same.

Circular Plate: Fig. 26 shows the resonance frequency of the first two modes of the plane in terms of the radius of the circular plate (R) and for different chemical potentials (μ_c). As it is known, the resonance of both modes decreases with increasing plate radius with the same slope, and the effect of increasing the chemical potential, similar to a rectangular plate, will lead to an increase in resonance. Triangular Plate: Fig. 27 shows the resonance frequencies of the first two modes of the plate in terms of the ratio of base (a) to the height (h) of the triangular plate and for different chemical potentials (μ_c). As can be seen from the diagrams, with increasing the base-to-height ratio, the resonant frequency of the first mode increases as long as the ratio of the base to the height is less than one, and the resonant frequency of the second mode increases as long as the

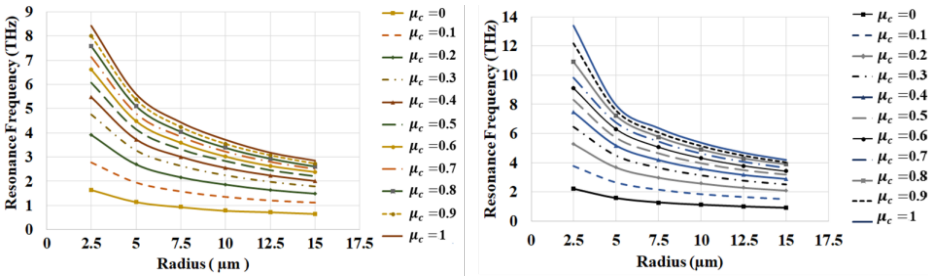

(a) (b)

Fig. 26. Resonance frequencies of the circular graphene plate as a function of plate radius for (a) the first mode, (b) the second mode

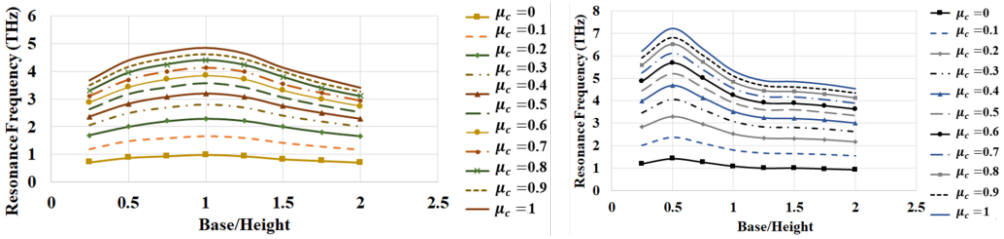

(a) (b)

Fig. 27. Resonance frequencies of the triangular graphene plate as a function of the ratio of the base to height for (a) the first mode, (b) the second mode

ratio of the base to the height is less than 0.5. By crossing the limit of 0.5 for the ratio of base to height, the trend of resonant frequencies changes of the second mode decreases and by crossing the limit of 1 for this ratio, the trend of resonant frequency changes of the first mode also decreases. In fact, by comparing the shape of the distribution of currents on a triangular plane with a constant height and different bases, shown in Figs. 13 to 15, we can change the maximum location of the first mode current from the vertex of the triangle to the base of the triangle by increasing the size. This trend is reversed for the second mode, so by crossing the border of 1 or 0.5, ascending section of the graphs changes to a descending part. In order to better show the effect of plate dimensions and chemical potential on the resonance frequencies of its first two modes, a function extracted using the curve fitting method for each resonance frequency. These functions that have been summarized in Table 3, can be used in designing and analyzing of graphene rectangular or circular patch antennas. As can be seen from the proposed function, in all plates the resonance frequency of both modes is approximately proportional to $\sqrt{\mu_c}$. From the proposed function, it is clear that for a rectangular plate, the effect of the plate length on the first mode is greater and the effect of the plate width on the second mode is greater.

For a circular plane, the effect of the radius of the circle on both modes is the same, and the resonant frequency of both modes is approximately proportional to $1\sqrt{R}$.

B.4. THE EFFECTS OF PEC GROUND PLANE

In order to investigate the effect of the presence of the ground plane on the characteristic modes, the mentioned graphene rectangular plate was placed at the height of h = 2 μm on top of a perfect electric conductor plate with dimensions of 25μm × 17.5μm, as shown in Fig. 28. The results for the eigenvalue, the modal significance, and the characteristic angle in terms of frequency, for the first two modes of the mentioned structure and for $\mu_c = 0.5\ eV$ and $h = 2\ \mu m$ are shown in Figs. 29 to 31. The current distribution of the first 6 modes at the corresponding resonant frequencies is also shown in Fig. 32. for a better comparison, the resonance frequency and the radiation bandwidth of the first six modes of this structure and the structure without a ground plane are summarized in Tables 4 and 5. As it turns out, the presence of a ground plane has no effect on the current distribution of the modes, but it does reduce the resonant frequencies and the radiation bandwidth. It can also be seen that the metal earth plane itself has a first mode with a resonance of about 5.5THz, which is not a problem for chemical potentials where the graphene plate resonance is far from the ground resonance, and the effect on graphene modes is small, but for larger chemical potentials graphene resonance, will approach the metal ground and it will be difficult to separate these modes from each other. For example for the state with $\mu_c = 0.5\ eV$, the first and second modes of the metal plate have resonance frequencies at 5.6THz and 9.5THz, and the current distribution of these two modes on the metal earth plate is shown in Fig. 33. To confirm the resonances obtained for the first two modes for $\mu_c = 0.5\ eV$, the mentioned structure is simulated with a feed line in CST software and analyzed in full wave. Depending on the shape of the current distribution, which is the maximum at horizontal edge for the first mode and maximum at the vertical edges for the second mode, the feed line is applied once to the vertical edge (width of the patch) and once to the horizontal edge (length of the patch), respectively. This stimulate the first and second modes, respectively. The structure of feed line and current distribution of the first and second modes can be seen in Fig. 34., and the return loss diagram of each mode can be seen in Fig. 35. The resonant frequency of the first mode is about 3.3 THz and the resonance of the second mode is about 4.2 THz, and is close to the values obtained in the mode analysis by FEKO software. Studies show that the presence of a metal ground plane under the graphene plate will generally change the resonance frequencies. By changing the dimensions of the ground plane, it was found that the dimensions of the ground plane do not have much effect on the resonance frequency of the modes, so only the change in height has been studied.

It should be noted that although the dimensions of the ground plane have little effect on the resonances of the graphene plate, but due to the difference between the material of the earth plate which is metal and the material of the graphene plate, if the earth dimensions are too large,

Table 4. The resonance frequencies of the first six modes of the rectangular plate on the PEC ground plane in comparison with the rectangular plate without ground plane

	The resonance frequency (THz)					
	Mode 1	Mode 2	Mode 3	Mode 4	Mode 5	Mode 6
Without ground plane	3.5	4.52	4.92	5.92	6.41	7.29
With ground plane	3.21	4.27	4.77	5.71	6.29	7.18

Table 5. The radiation bandwidth of the first six modes of the rectangular plate on the PEC ground plane in comparison with the rectangular plate without ground plane

	The radiation bandwidth (THz)					
	Mode 1	Mode 2	Mode 3	Mode 4	Mode 5	Mode 6
Without ground plane	5.7	5.1	3	2.7	2.5	2.2
With ground plane	4.98	3.75	3.35	2.8	2.38	1.81

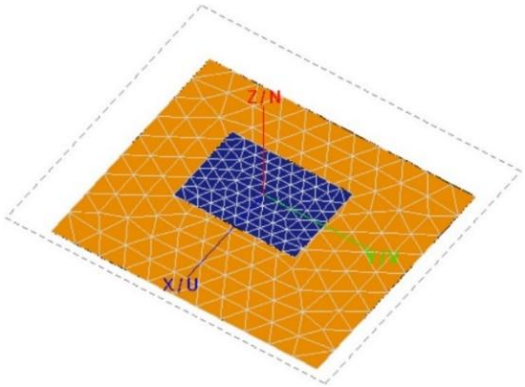

Fig. 28. The graphene plate on the PEC ground plane

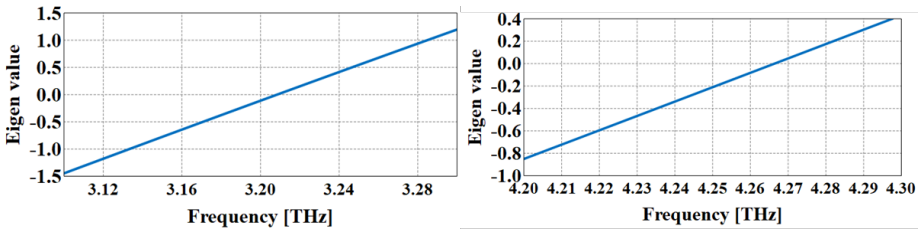

Fig. 29. The eigenvalue, of the rectangular graphene plate on the PEC ground plane, a) the first mode, b) the second mode

its resonance frequencies decrease to the terahertz range and will affect the resonances of the graphene plate, and even if the dimensions of the ground are very small, it is unrealistic and will not show its effect.

Therefore, the dimensions of the ground plane were fixed to 25μm × 17.5μm to investigate the effect of height, which is two and a half times greater than the graphene plate. In order to better investigate the effect of the distance between the metal ground plane and the graphene plate, the

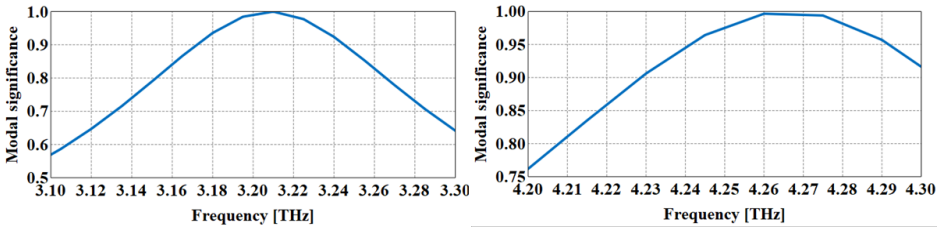

(a) (b)

Fig. 30. The modal significance, of the rectangular graphene plate on the PEC ground plane, a) the first mode, b) the second mode

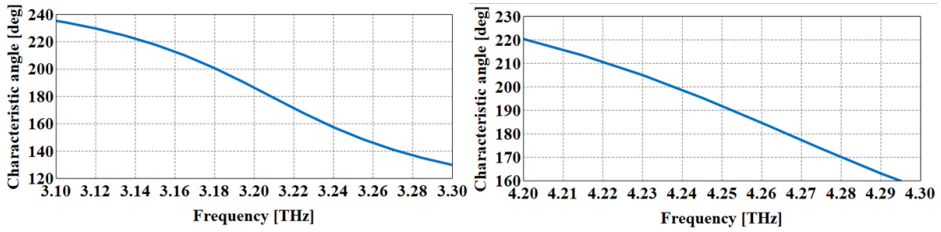

(a) (b)

Fig. 31. The characteristic angle, of the rectangular graphene plate on the PEC ground plane, a) the first mode, b) the second mode

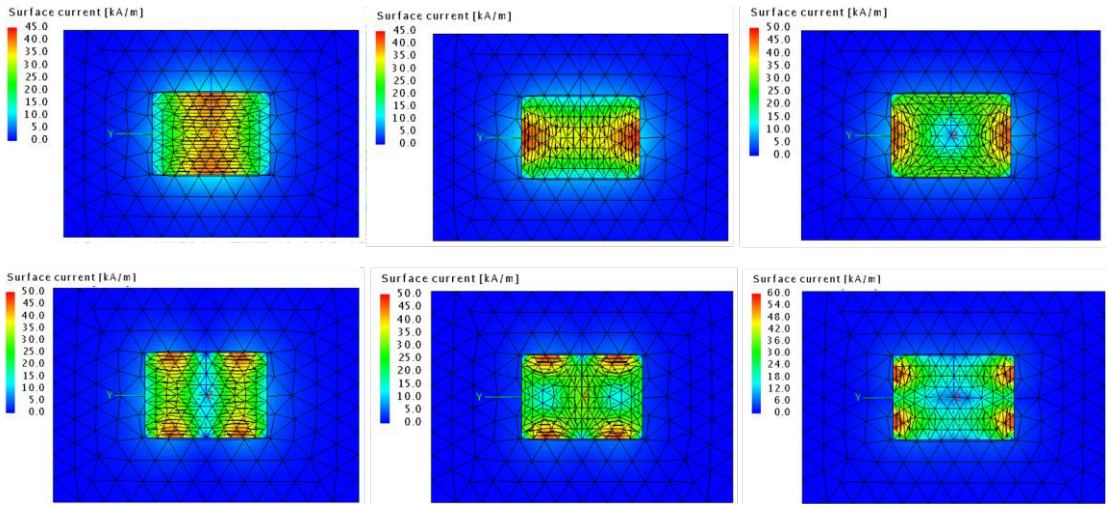

Fig. 32. The current distribution at the resonance frequencies of the first six modes of the rectangular plate on the PEC ground plane

diagrams in Fig. 36. were drawn, which show the resonance frequency of the first two modes of the structure in terms of distance h and for different chemical potentials.

As can be seen, with increasing the height of the resonance of both modes has increased somewhat, but the slope of this increase is very low for both modes, so it can be said that the height has little effect on the resonance frequency of the modes. In order to be able to consider the effect of the height parameter in designing of graphene patch antenna and calculate the resonance

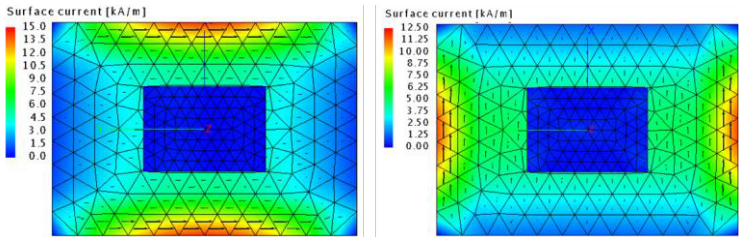

Fig. 33. The current distribution at the resonance frequencies of the first two modes of the PEC ground plane under the graphene plate

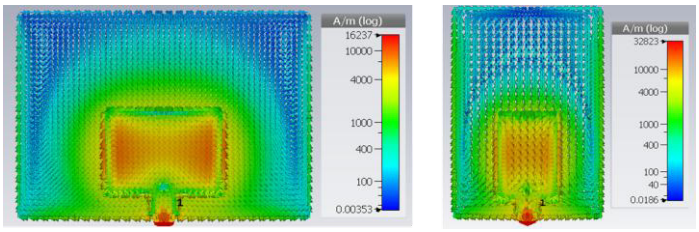

(a) (b)

Fig. 34. The current distribution at the resonance frequencies of the first two modes of the rectangular graphene plate on the PEC ground plane, a) horizontal feeding, b) vertical feeding

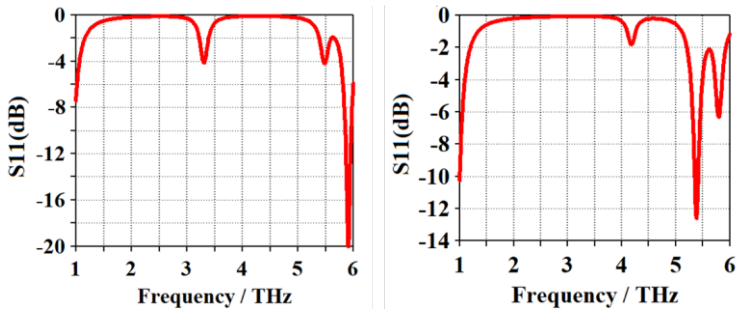

(a) (b)

Fig. 35. The $|S_{11}|$ diagram of the structure of the rectangular graphene plate on the PEC ground plane with $\mu_c = 0.5\ eV$, a) horizontal feeding, b) vertical feeding

Table 6. Resonance frequency function of the first two modes of rectangular graphene plate on the PEC ground plane according to the chemical potential of graphene and height of the graphene plate from the ground plane

The resonance frequency of the first mode(THz)	The resonance frequency of the second mode(THz)
$f_{r1}(\mu_c, h) = 4.02\ \mu_c^{0.47} h^{0.11}$	$f_{r2}(\mu_c, h) = 5.45\ \mu_c^{0.47} h^{0.085}$

frequency by considering the chemical potential and by changing h by extracting, two functions which are summarized in Table 6, extracted related to the diagrams in Fig. 36. These functions can be used for calculating resonance frequencies of the first and second modes in terms of the chemical potential of graphene and the height of the graphene plate relative to the metal earth plate.

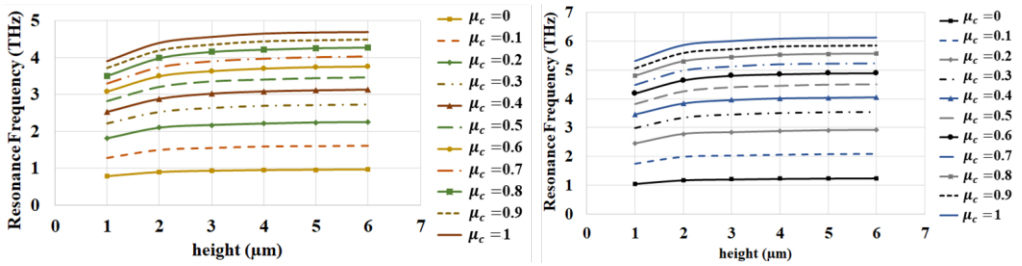

(a) (b)

Fig. 36. Resonance frequencies of rectangular graphene plate on PEC ground plane as a function of height, a) the first mode, b) the second mode

IV. CONCLUSION

In this paper, characteristic mode analysis for graphene plates was performed and the effect of graphene chemical potential, relaxation time and the dimension of the plates on the behavior of characteristic modes of these structures, especially on the first and second modes, was investigated. Also, the effect of the presence of the ground plane and its height on the resonance frequency of the modes was studied. The relationship between the resonant frequency of the first two modes of graphene plates and the dimensions of the plate and the chemical potential parameter of graphene were extracted as power functions. The mentioned functions can be used in calculating the resonance frequency of graphene plates and in designing antennas. The summary of the results obtained from this analysis includes the following: Graphene plates with micrometer dimensions have resonances in the terahertz frequency range that are much lower than the resonant frequencies of metal plates of the same dimensions as the graphene plate. As the chemical potential of graphene increases, the resonance frequency of the first two modes of graphene plates increases with a relatively equal slope. In all graphene plates, the resonance frequency of both modes is approximately proportional to $\sqrt{\mu_c}$. For a rectangular plate, the first mode is affected by the length of the plate and the second mode by the width of the plate. The presence of a metal ground reduces the radiation bandwidth of the modes. The novelty of this work lies in providing the first systematic CMA-based framework for analyzing graphene plates of different shapes, extracting the influence of chemical potential, relaxation time, and geometrical parameters on the modal behavior, and deriving analytical power functions to accurately predict the resonance frequencies of the first two modes. Unlike previous studies that relied solely on full-wave simulations, the results presented here offer generalized physical insights and practical design equations that enable graphene antenna designers to estimate resonance frequencies without the need for extensive numerical simulations.

REFERENCES

[1] Y. Dong, P. Liu, D. Yu, G. Li and F. Tao, "Dual-Band Reconfigurable Terahertz Patch Antenna with Graphene-Stack-Based Backing Cavity," *IEEE Antennas and Wireless Propagation Letters*. vol. 15, pp. 1541-1544, 2016.

[2] A. Cabellos-Aparicio, I. Llatser, E. Alarcón, A. Hsu, T. Palacios, "Use of Terahertz Photoconductive Sources to Characterize Tunable Graphene RF Plasmonic Antennas," *IEEE Trans. Nanotechnology*. vol. 14, no. 2, pp. 390-396, March 2015.

[3] T. Li and Z. N. Chen, "A Dual-Band Metasurface Antenna Using Characteristic Mode Analysis," *IEEE Trans. Antennas and Propagation*. vol. 66, no.10, pp. 5620-5624, Oct. 2018.

[4] M. Cabedo-Fabres, E. Antonino-Daviu, A. Valero-Nogueira, and M. F.Bataller, "The theory of characteristic modes revisited: a contribution to the design of antennas for modern applications," *IEEE Antennas Propag. Mag.* vol. 49, no. 5, pp. 52–68, Oct. 2007.

[5] S. Dey, D. Chatterjee, E. J. Garboczi and A. M. Hassan, "Plasmonic Nanoantenna Optimization Using Characteristic Mode Analysis," *IEEE Trans. Antennas and Propagation*, vol. 68, no. 1, pp. 43-53, Jan. 2020.

[6] C. Chunling, "Characteristic mode analysis and design of a slot-loaded low-profile wideband microstrip patch antenna," *Microw Opt Technol Lett*., vol. 62, pp. 1374– 1379, March 2020.

[7] M. B. Perotoni, F. A. A. da Silva, L. A. da Silva, "Characteristic Mode Analysis applied to antennas," *Revista Brasileira de Ensino de Física*, vol. 42, e20200119, 2020.

[8] N. Sathishkumar, S. Palanisamy, R. Natarajan, K. Ouahada, and H. Hamam, "Design of dual mode antenna using CMA and broadband dual-polarized antenna for 5G networks," *Scientific Reports*, vol. 14, no. 1, p. 15553, July 2024.

[9] U. Ullah, S. Koziel, and A. Pietrenko-Dabrowski, "Characteristic mode analysis and excitation of orthogonal modes on a single substrate for wideband IoT applications in the millimeter wave band," *Scientific Reports*, vol. 15, p. 8810, 2025.

[10] I. B. Sharma, P. Joshi, S. Shrimal, B. Kalra, and M. M. Sharma, "The design of multi band antenna with improved higher order mode radiation using CMA for L5-band, L1-band, and S-band application," *Scientia Iranica*, online Nov. 26, 2023.

[11] B. G. P. Shariff, S. Pathan, P. R. Mane, *et al.*, "Characteristic mode analysis based highly flexible antenna for millimeter wave wireless applications," *Journal of Infrared, Millimeter, and Terahertz Waves*, vol. 45, pp. 1–26, 2024.

[12] B. R. Perli, K. J. Babu, T. Addepalli, M. K. Kumar, J. P. Kumar, M. V. Sudhakar, *et al.*, "Characteristic modes analysis of CPW-fed UWB monopole antenna for short-distance wireless communications," *Telecommunications and Radio Engineering*, vol. 84, no. 8, pp. 1–14, 2025.

[13] G. Kyriakou, P. Bolli, and G. Virone, "Characteristic Modes Analysis of Mutually Coupled Log-Periodic Dipole Antennas," *arXiv preprint arXiv: 2304.00332*, Apr. 2023.

[14] M. A. Gaber, M. El-Aasser, A. Yahia, *et al.*, "Characteristic modes of a slot antenna design based on defected ground structure for 5G applications," *Scientific Reports*, vol. 13, p. 15327, 2023.

[15] Chen, Y. and C.-F. Wang, Characteristic modes: Theory and applications in antenna engineering, John Wiley & Sons 2015.

[16] R. Harrington, J. Mautz, "Theory of characteristic modes for conducting bodies," *IEEE Trans. Antennas Propag*, vol. 19, no. 5, pp. 622-628, Sept. 1971.

[17] S. Anand , M. Thampy, D. S. Sudesh, "Analysis of graphene based optically transparent patch antenna for terahertz communications," *Physica E: Low-dimensional Systems and Nanostructures*. vol. 66, pp. 67-73, 2015.

[18] S. N. Hafizah Sa'don, M. H. Jamaluddin, M. R. Kamarudin, F. Ahmad, Y. Yamada, K. Kamardin and I. H. Idris, "Analysis of Graphene Antenna Properties for5 G Applications," Sensors, vol. 19, p. 4835, 2019.

[19] K. Q. da, G. T. Conde, and G. S. Pinto, "Numerical Analysis of Broadband Dipole-Loop Graphene Antenna for Applications in Terahertz Communications," *Antennas and Wave Propagation*. London, United Kingdom: Intech Open, 2018 [Online].

[20] C. Suessrneier, S. Abadal, L. Banszerus, F. Thiel, E. Alarcón, A. K. Wigger, A. Cabellos-Aparicio, C. Stampfer, M. Lemme and P. H. Bolívar, "Analysis of a Plasmonic Graphene Antenna for Microelectronic Applications," *43rd International Conference on Infrared, Millimeter, and Terahertz Waves (IRMMW-THz)*, 1-2, 2018.

[21] M. Feizi, V. Nayyeri and O. M. Ramahi, "Modeling Magnetized Graphene in the Finite-Difference Time-Domain Method Using an Anisotropic Surface Boundary Condition," *IEEE Trans. Antennas and Propagation*, vol. 66. no. 1, pp. 233-241, Jan. 2018.

[22] K. Niu, P. Li, Z. Huang, L. J. Jiang and H. Bagci, "Numerical Methods for Electromagnetic Modeling of Graphene: A Review," *IEEE Journal on Multiscale and Multiphysics Computational Techniques*, vol. 5, pp. 44-58, 2020.

[23] G. L. P. Ashok, G. V. Nath, and B. C. Neelapu, "Graphene-enhanced decagonal patch antenna for terahertz frequency operation in breast cancer detection," *Applied Optics*, vol. 63, pp. 3609–3618, 2024.

[24] M. Mashayekhi, P. Kabiri, A. S. Nooramin, *et al.*, "A reconfigurable graphene patch antenna inverse design at terahertz frequencies," *Scientific Reports*, vol. 13, p. 8369, 2023.

[25] S. O. Hasan, S. K. Ezzulddin, H. A. Khizir, *et al.*, "Design of graphene-based tunable plasmonic antenna for multiband terahertz application systems," *Plasmonics*, vol. 19, pp. 2107–2118, 2024.

[26] M. F. F. Mukhtar, N. Bahari, H. A. Rahim, and M. H. Mat, "Design and analysis of graphene-based antenna using various substrate materials for 6G applications," in *2024 IEEE 1st International Conference on Communication Engineering and Emerging Technologies (ICoCET)*, Kepala Batas, Penang, Malaysia, pp. 1–4, 2024.

[27] S. Ullah, I. Marasco, A. D'Orazio, *et al.*, "Graphene-based programmable dual dipole antenna with parasitic elements," *Optics and Quantum Electronics*, vol. 57, p. 142, 2025.

[28] K. Moradi, A. Pourziad, S. Nikmehr, "Reconfigurable characteristics of graphene plates," *Appl. Opt*. vol. 58, no. 20, pp. 5415–5421, 2019.

[29] K. C. Durbhakula, A. M. Hassan, F. Vargas-Lara, D. Chatterjee, M. Gaffar, J. F. Douglas, and E. J. Garboczi, "Electromagnetic scattering from individual crumpled graphene flakes: a characteristic modes approach," *IEEE Trans. Antennas Propag*. vol. 65, no. 11, pp. 6035–6047, Nov. 2017.

[30] C. R. Peñafiel-Ojeda, M. Cabedo-Fabrés, A. Llanga-Vargas and M. Ferrando-Bataller, "Low-profile UWB antenna with unidirectional radiation pattern analyzed with the theory of characteristic modes*," AEU - International Journal of Electronics and Communications.* vol. 142, 153981, Dec. 2021.

[31] B. Zhang, J. Zhang, C. Liu and Z. P. Wu, "Input Impedance and Efficiency Analysis of Graphene-Based Plasmonic Nanoantenna Using Theory of Characteristic Modes," *IEEE Antennas and Wireless Propagation Letters*. vol. 18, no. 10, pp. 2031-2035, 2019.

[32] K. Moradi, A. Pourziad, and S. Nikmehr, "Characteristic mode analysis of graphene based patch antenna in terahertz regime," *Arabian Journal for Science and Engineering*, vol. 49, pp. 7245–7257, 2024.

[33] H. A. Malhat, and S.H. Zainud-Deen*,* "Equivalent circuit with frequency-independent lumped elements for plasmonic graphene patch antenna using particle swarm optimization technique," *32nd National Radio Science Conference (NRSC),* 2015.

[34] O. Kyung Suk and J.E. Schutt-Aine, "An efficient implementation of surface impedance boundary conditions for finite-difference time-domain method," *IEEE Trans. Antennas and Propagation*, vol. 43, no.7, pp. 660-666, July 1995.

[35] J. C. C. Mak, and C.D. Sarris, "A surface impedance boundary condition approach to the FDTD modeling of graphene," in *2013 IEEE Antennas and Propagation Society.*

Journal of Communication Engineering (JCE)